Comput Mech (2010) 45:623–635
DOI 10.1007/s00466-010-0475-3

ORIGINAL PAPER

Extended multiscale finite element method for elasto-plastic analysis of 2D periodic lattice truss materials

H. W. Zhang · J. K. Wu · Z. D. Fu

Received: 2 November 2009 / Accepted: 19 January 2010 / Published online: 10 February 2010

Abstract An extended multiscale finite element method is developed for small-deformation elasto-plastic analysis of periodic truss materials. The base functions constructed numerically are employed to establish the relationship between the macroscopic displacement and the microscopic stress and strain. The unbalanced nodal forces in the microscale of unit cells are treated as the combined effects of macroscopic equivalent forces and microscopic perturbed forces, in which macroscopic equivalent forces are used to solve the macroscopic displacement field and microscopic perturbed forces are used to obtain the stress and strain in the microscale to make sure the correctness of the results obtained by the downscale computation in the elastic-plastic problems. Numerical examples are carried out and the results verify the validity and efficiency of the developed method by comparing it with the conventional finite element method.

Keywords Truss material · Elasto-plastic analysis · Extended multiscale finite element method · Base function

1 Introduction

As a result of the rapid developments in manufacturing techniques recently, there is growing interest in the study of lattice truss material, which is composed of periodic unit cells that can be decomposed in elementary bars (Fig. 1). This kind of material is widely used in civil engineering [1] and aeronautic engineering structures [2,3] due to its excellent performance such as high stiffness-weight, high strength-weight ratios and easy of construction. These advantages make it as one of most attractive ultra-light materials. Deshpande et al. [4] demonstrated that stretching-governed lattice truss materials are much stiffer and stronger than bending-governed foamed materials; thus, this material may substitute for metallic foams in lightweight structures.

When the truss material structure involves multiple spatial scales, the material behavior is influenced by the physical phenomena which take place at each scale and by the interaction of the phenomena across scales. In this context, the direct numerical solutions on the whole structure by meshing all heterogeneities may be not practicable even using the advanced supercomputers, owing to the requisite of tremendous amount of computer memory and CPU time. An effective way to overcome this difficulty is to develop multiscale algorithms that can be used to obtain the equivalent material model. Considerable research works have already been done to predict equivalent elastic property [6–11] and dynamic model [12,13] of complicated periodic materials, and have achieved significant results. It is clear that robust fundamental studies about damage and failure mechanisms are important for designing advanced materials in high performance applications. However, there are a few restrictions when the aforementioned methods are applied to solve nonlinear problems, since most of the theories developed for finding effective material properties do not pay much attention to the accurate evaluation of the microscopic variables in the framework of nonlinear analysis.

In recent years, a considerable amount of effort has been made on developing multiscale algorithm for solving

H. W. Zhang (✉) · J. K. Wu · Z. D. Fu
State Key Laboratory of Structural Analysis for Industrial Equipment, Department of Engineering Mechanics, Faculty of Vehicle Engineering and Mechanics, Dalian University of Technology, Dalian 116024, People's Republic of China
e-mail: zhanghw@dlut.edu.cn

J. K. Wu
e-mail: jingkaiwu@student.dlut.edu.cn

Z. D. Fu
e-mail: fzhd@student.dlut.edu.cn

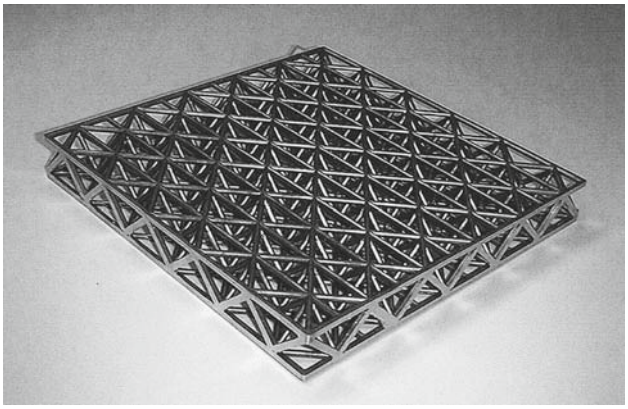

Fig. 1 Photograph of 3D truss material made from an aluminum casting alloy [5]

nonlinear problems. Notable among the recent developments is the asymptotic homogenization theory which was first proposed by Benssousan et al. [14]. In this method, the FEM is applied to yield the homogenized material parameters as well as evaluate the actual stress field in a microscale from the macroscopic responses [15]. Since the method has the ability to evaluate the microscopic variables within the unit cells, it has been extended to solve various nonlinear multiscale problems: the evaluation of local damage [16,17], small deformation elastoplastic problems [18–20], etc. Though the asymptotic homogenization methodologies have been successfully used for solving the heterogeneous elasto-plastic problems, they do have some shortcomings. Besides local periodicity hypothesis, these methods request that the ratio between the small-scale length and the large-scale length is very small. Moreover, for nonlinear history dependent systems, since the microscopic problems are solved at each macroscopic (Gauss) point of the FE mesh, the deformation histories have to be stored and updated at all integration points, that is to say, the current multiscale method still require enormous computational efforts in practical applications when the structures are large [19,21,22].

The multiscale finite element method (MsFEM) takes their origin from a pioneering work of Babuska and Osborn [23,24] and is extended to the general heterogeneities by Hou and Wu [25]. It provides an effective way to capture the large-scale solutions on a coarse-scale mesh without resolving all the small-scale features. This is accomplished by constructing the multiscale base functions that are adaptive to the local property of the differential operator. The small scale information is then brought to the large scales through the coupling of the global stiffness matrix, and the effect of small-scales on the coarse-scales is correctly captured. The MsFEM has been widely used for numerically solving second order elliptic boundary value problems with high oscillating coefficients since it was proposed. For example: the method has been generalized and successfully used for simulation of two-phase flow and transport in highly heterogeneous porous media [26–29]. Recently, Dostert et al. [30] investigated the MsFEM for stochastic permeability field as well as application to uncertainty quantification. Moreover, several similar multiscale methods have been developed, such as the multiscale finite volume method (MsFV) [31] and the multiscale finite volume element method (MsFVEM) [32].

However, less literature has discussed about the applications of the MsFEM for vector field problems of computational solid mechanics. Reference [33] seems the first one in which the MsFEM was developed for solving the coupling problems of consolidation of heterogeneous saturated porous media under external loading conditions. In this method, two sets of base functions are constructed, respectively, for the coarse-scale model. One set is for the pressure field of fluid flow and the other is for the displacement field of solid skeleton. Our recent research [34] has found that the base function constructed in [33] for solid phase cannot capture well the small-scale deformation information in the unit cell due to Poisson's effect. Thus, the coupled additional terms of base function for the interpolation of the displacement field are introduced in the extended multiscale finite element method (EMsFEM) [34] to consider the coupled effect among different directions in the multi-dimensional problems. The results in [34] show that the EMsFEM can be successfully used for solving elastic multiscale problems of periodic truss material. Meanwhile, the method can execute the downscaling computation easily and the actual micro stress and strain within the unit cells can be obtained simultaneously in the multiscale computation. Thus the EMsFEM has great potential for strength analysis of heterogeneous materials.

The objective of this paper is to extend the EMsFEM proposed in [34] for elastic problems to small deformation elasto-plastic problems of periodic truss materials. In the present method, the unbalanced nodal forces in the microscale of unit cells are treated as the combined effects of macroscopic equivalent forces and microscopic perturbed forces, in which macroscopic equivalent forces are used to solve the macroscopic displacement field and microscopic perturbed forces are used to obtain the stress and strain in the microscale to make sure the correctness of the results obtained by the downscale computation in the elastic-plastic problems. Then, the modified Newton–Raphson iterative method is introduced for solving micro- and macro-structure. The numerical experiments show that the results obtained by the EMsFEM agree well with the reference solutions for elastic-plastic analysis of periodic truss materials. Meanwhile, the CPU time and memory storage can be reduced drastically.

It should be remarked that, unlike other homogenization methods, the microscopic problems in our method are solved

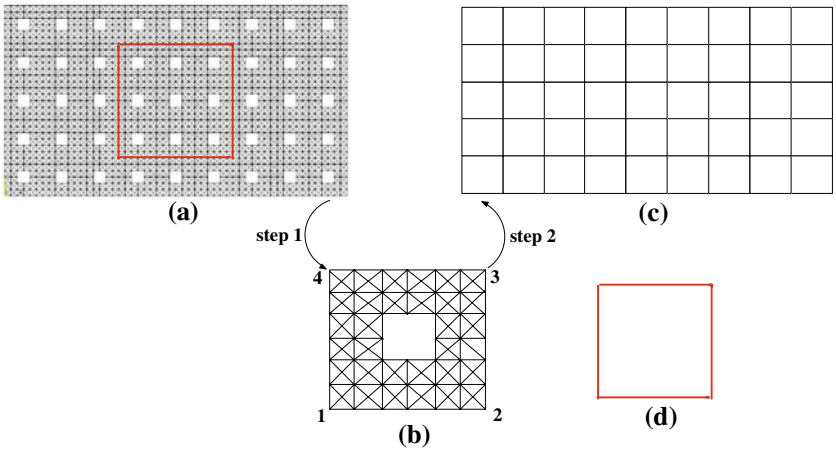

Fig. 2 Illustration of the EMsFEM: **a** Truss material structure with periodic microstructure; **b** The truss unit cell; **c** The coarse-scale (macroscopic) meshes of the model and **d** the sampling element

on macroscopic elements directly rather than at Gauss points of the elements. Thus, the computational cost is further reduced and the ratio between the small-scale length and the large-scale length is not restricted here. Moreover, for EMsFEM, the construction of base functions and downscaling computations are performed in each macroscopic element independently, that is to say, the method developed here can be extended for the parallel computing in simple way as well as strength analysis of non-periodic continuum problems.

This paper is organized as follows: in the next section, we summarize the formulation of the EMsFEM proposed in [34], which is used for elastic problems of periodic truss material. In Sect. 3, the equivalence technique of microscopic nodal forces in multiscale frame is presented. Thus, the technique can be used for treatment of the microscopic unbalanced nodal forces in nonlinear computation. In Sect. 4, some fundamental formulations used in elasto-plastic computation are provided, and then the flow chart of iteration process is given in the framework of two-scale elasto-plastic analysis. In Sect. 5, several simple, but illustrative numerical examples are conducted and compared with direct FE method to examine the validity of the EMsFEM for nonlinear problems. At the same time, two kinds of boundary conditions which are used for the construction of base functions are compared. In Sect. 6, the memory storage and computing time are compared between the EMsFEM and the traditional FEM to show the efficiency of our method. Finally, some discussions are presented.

2 EMsFEM for elastic analysis of periodic truss material

In this section, we briefly summarize the EMsFEM for elastic analysis of periodic truss material with reference to Zhang et al. [34]. After presenting the derivation process of the formulas for micro- and macro-scale computation, we also illustrate downscaling algorithm for computing microscopic stress and strain information which can be used for elasto-plastic analysis in the following sections.

Consider a heterogeneous truss material structure occupying a region $\Omega_{\text{structure}}$ depicted in Fig. 2a, which is composed of periodic truss unit cells as shown in Fig. 2b. The structure is subjected to a system of external forces F_{ext}, and prescribed displacement fields on the boundary Γ_u. There are two computational steps need to be performed for the EMsFEM (see Fig. 2). One is micro-scale computation in which the multiscale base functions of the unit cell are constructed and the equivalent stiffness matrix is derived. The other is macro-scale computation, in this step, the FEM are handled on the coarse meshes (shown in Fig. 2c) since the unit cell's equivalent stiffness matrix has been obtained. Note that the sizes of coarse meshes used in EMsFEM are as large as those of unit cells.

2.1 Micro-scale computation

2.1.1 The construction of base functions of unit cell

In the EMsFEM, the main work is to construct the base functions of unit cells numerically, whose values can capture well the small-scale heterogeneities of unit cells. The base functions are constructed by solving the equilibrium equation on each fine-scale mesh within the unit cell with special boundary conditions. Reference [34] has introduced two kinds of boundary conditions, i.e., the linear boundary condition and the oscillatory boundary condition, to construct base functions.

Firstly, let's take the linear boundary condition as an example to illustrate the construction process of base functions. For the vector field problems of computational solid mechanics, the base functions must be constructed separately for each coordinate direction. In 2D problems, two kinds of base functions for interpolation of the displacement field of the truss structures are needed to constructed, in which one is used for

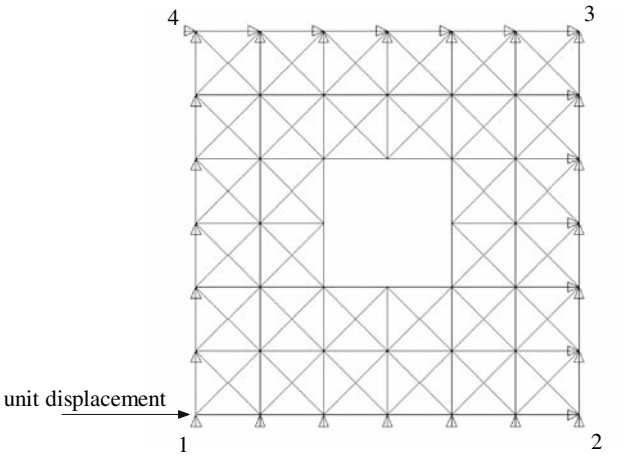

Fig. 3 The construction of base functions for truss cell

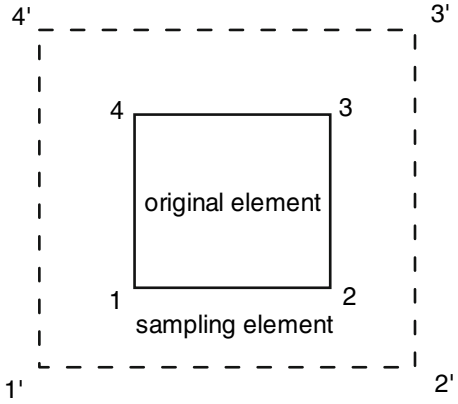

Fig. 4 Illustration of the oversampling technique

the displacement interpolation in x-direction and the other is used for y-direction. Firstly, let us consider the construction of N_{1x}. For the unit cell shown in Fig. 3, the displacements at all boundary nodes are constraint in y direction. At the same time, the nodes on boundary 34 and boundary 23 are constraint in x direction to avid rigid displacement. For the linear boundary condition, a unit displacement is applied on node 1 in x-positive direction, and the values vary linearly along boundaries 12 and 14, just as in the standard bilinear (linear) base functions. Using the boundary condition mentioned above, the internal displacement field of unit cell can be obtained directly by standard finite element analysis in fine-scale mesh, and the base functions N_{1x} and N_{1xy} can be obtained. Here, N_{ixy} is a coupled additional term and means that the displacement field in y direction within the unit cell induced by unit displacement of node i in x direction. The rest of base functions can be constructed in the similar way.

It can been verified that the base functions constructed above satisfy

$$\begin{cases} \sum_{i=1}^{4} N_{ix} = 1, \quad \sum_{i=1}^{4} N_{iy} = 1 \\ \sum_{i=1}^{4} N_{ixy} = 0, \quad \sum_{i=1}^{4} N_{iyx} = 0 \end{cases} \tag{1}$$

which ensures the rigid displacement of unit cell and the compatibility between the neighboring unit cells.

Another more appealing approach is to construct the oscillatory boundary condition for the construction of base functions using the oversampling technique. Consider a larger domain that covers the unit cell as illustrate in Figs. 2d and 4, in which $\Delta 1234$ is the original element (unit cell) and $\Delta 1'2'3'4'$ is the sampling element. Firstly, temporary base functions $\psi_{j'}(j' = 1', 2', 3', 4')$ are constructed with linear boundary method presented above. Then the temporary base functions ϕ are constructed from the linear combination of ψ as follows

$$\phi_i = \sum_{j=1}^{4} c_{ij}\psi_{j'}, \ (i = 1, 2, 3, 4) \tag{2}$$

where c_{ij} are the constants determined by the condition $\phi_i|_j = \delta_{ij}$, δ is the Kronecker delta.

It is noticed that the temporary base functions ϕ and ψ are only used to obtain the oscillatory boundary condition, so the coupled additional terms are not considered in the computation. The values of ϕ_i at unit cell's boundary can be called as oscillatory boundary condition from which the actual base functions $\mathbf{N}$ for the unit cell can be constructed. The final base functions, i.e. N_{ix}, N_{ixy}, N_{iy} and $N_{iyx}(i = 1, 2, 3, 4)$ obtained by this way also satisfy Eq. 1.

Thus, the displacement fields within the unit cell can be expressed as

$$u = \sum_{i=1}^{4} N_{ix}u'_i + \sum_{i=1}^{4} N_{iyx}v'_i \tag{3}$$

$$v = \sum_{i=1}^{4} N_{iy}v'_i + \sum_{i=1}^{4} N_{ixy}u'_i \tag{4}$$

which can be given in a unified form

$$\mathbf{u} = \mathbf{N}\mathbf{u}'_{\mathbf{E}} \tag{5}$$

where $\mathbf{N}$ is the base function matrix of the unit cell, $\mathbf{u}$ is the nodal displacement vector in the micro scale, and $\mathbf{u}'_{\mathbf{E}}$ is the nodal displacement vector of the unit cell in macro scale. They can be expressed as

$$\mathbf{u} = \left[u_1 \ v_1 \ u_2 \ v_2 \cdots u_n \ v_n \right]^{\mathrm{T}} \tag{6}$$

$$\mathbf{N} = \left[R_x(1)^{\mathrm{T}} \ R_y(1)^{\mathrm{T}} \ R_x(2)^{\mathrm{T}} \ R_y(2)^{\mathrm{T}} \cdots R_x(n)^{\mathrm{T}} \ R_y(n)^{\mathrm{T}} \right]^{\mathrm{T}} \tag{7}$$

$$\mathbf{u}'_{\mathbf{E}} = [\, u'_1 \ v'_1 \ u'_2 \ v'_2 \ u'_3 \ v'_3 \ u'_4 \ v'_4 \,]^{\mathrm{T}} \tag{8}$$

where

$$R_x(i) = [N_{1x}(i)N_{1yx}(i)N_{2x}(i)N_{2yx}(i)N_{3x}(i)N_{3yx}(i) \quad N_{4x}(i)N_{4yx}(i)] \tag{9}$$
$$R_y(i) = [N_{1xy}(i)N_{1y}(i)N_{2xy}(i)N_{2y}(i)N_{3xy}(i)N_{3y}(i) \quad N_{4xy}(i)N_{4y}(i)]$$

and n is the total number of the micro nodes in the unit cell.

2.1.2 Equivalent stiffness matrix of the truss unit cell

Once the base functions are constructed, the equivalent stiffness matrix of unit cell can be obtained in the following form:

$$\mathbf{K}_E = \sum_{i=1}^{M} \mathbf{G^{ei}}^{\mathbf{T}} k_e^i \mathbf{G^{ei}} \tag{10}$$

where M is the total number of micro truss elements in the unit cell, and $k_e = \frac{EA}{l}$ is elastic coefficient of truss element, in which E is the Young's modulus, A is the element cross-sectional area and l is the length of the element, the transformation matrix $[\mathbf{G^{ei}}]$ is given by

$$[\mathbf{G^{ei}}] = [\,-cos\theta_i \;\; -sin\theta_i \;\; cos\theta_i \;\; sin\theta_i\,] \begin{bmatrix} R_x(m) \\ R_y(m) \\ R_x(n) \\ R_y(n) \end{bmatrix} \tag{11}$$

where m and n are the nodes of ith micro element in the unit cell.

Reference [34] has pointed out that the equivalent stiffness matrix derived by the base functions which are constructed with oscillatory boundary condition can not satisfy rigid-body displacement completely. Thus, the eigenvalues modified method (EMM) [35] was introduced to modify the stiffness matrix.

For a more detailed derivation process, the reader is refered to [34].

2.2 Macro-scale computation

Up to now, we have got the unit cell's equivalent element stiffness matrix $\mathbf{K}_E$. Note that for periodic materials, the matrix $\mathbf{K}_E$ only need to be solved one time. Then, the global stiffness matrix is obtained as follows

$$\mathbf{K} = \underset{i=1}{\overset{m}{\mathbf{A}}} \mathbf{K}_{\mathbf{E}}^m \tag{12}$$

where $\mathbf{A}_{i=1}^m$ is a matrix assembled operator, and m is total number of coarse elements.

Thus, a classical FE analysis is carried out on coarse elements, and the macroscopic displacement vector is given by

$$\mathbf{U} = F_{ext}/\mathbf{K} \tag{13}$$

2.3 Downscaling computation for microscopic information

When the multiscale procedures are performed for elasto-plastic analysis, it is necessary to obtain at the same time the stress and strain response in the micro scale as well as the macro behavior of the entire structure. For the EMsFEM, the relation between the micro and macro scales is created through the base functions which are constructed numerically and can capture the micro scale heterogeneities within the unit cell. By virtue of this relation, the downscaling computation could be realized easily and the stress and strain in micro-scale can be obtained simultaneously in the multiscale computation.

For the EMsFEM whose base functions are constructed with linear boundary condition, the internal force of the ith truss element within the unit cell can be written as

$$\overline{F}_i^e = \frac{E_i A_i}{l_i} [\mathbf{G^{ei}}]_i \left\{\mathbf{u}_{\mathbf{E}}'\right\} \tag{14}$$

While for oscillatory boundary condition, as the equivalent stiffness matrix has been modified, we assume that the modified stiffness matrix and the original one have the following relationship:

$$\mathbf{K}_{\mathbf{E}}' = \mathbf{S}\mathbf{K}_{\mathbf{E}}\mathbf{S}^{\mathbf{T}} \tag{15}$$

where matrix $\mathbf{S}$ is obtained by solving 64 nonlinear equations iteratively and only need to be solved one time for the materials with periodic microstructure. In this case, the mapping relations between micro-scale nodes and macro-scale nodes (i.e., Eq. 11) of the unit cell have been changed, that is

$$\mathbf{G^{ei'}} = \mathbf{G^{ei}}\mathbf{S}^{\mathbf{T}} \tag{16}$$

Using Eqs. 14 and 16, we can get the internal force of the ith truss element within the unit cell as follows

$$\overline{F}_i^e = \frac{E_i A_i}{l_i} \left[\mathbf{G^{ei'}}\right] \left\{\mathbf{u}_{\mathbf{E}}'\right\} \tag{17}$$

3 Treatment of micro-scale nodal forces within unit cells for EMsFEM

In the macro-scale computation step discussed in Sect. 2, the FE analysis is performed on the coarse meshes. Thus, for the formula (13), all the external forces F_{ext} must be applied on the macroscopic nodes. However, it is inevitable that some external forces are acted on the nodes of micro-scale meshes within unit cells in practice. Specially, for elasto-plastic multiscale analysis, it will induce unbalance nodal forces in micro-scale meshes with the increase of loading step. In this section, the treatment of these micro-scale nodal forces in the EMsFEM will be discussed. Note that the material properties used in this section are linear elastic.

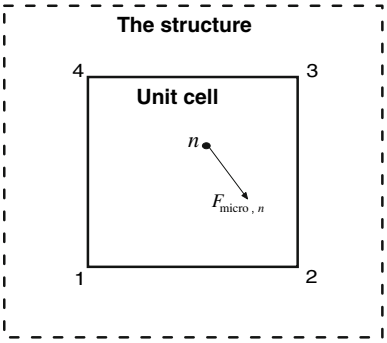

Fig. 5 A force applied on the node of microscale meshes of the unit cell which is contained in the structure

As shown in Fig 5, a force $F_{\text{micro},n}$ is applied on the nth node of micro-scale meshes of the unit cell which is contained in the structure. The problem here is how to substitute the macroscopic nodal forces (i.e., the forces applied on the corner node of unit cell) for the micro-scale nodal force, while the global displacement response of structure and local micro-scale stress and strain response within the unit cell are remain unchanged. In our method, the nodal forces in the micro-scale in unit cells are treated as the combined effects of macroscopic equivalent forces and microscopic perturbed forces (see Fig. 6), in which macroscopic equivalent forces are used to solve the macroscopic displacement field and microscopic perturbed forces are used to obtain the stress and strain in the micro-scale. We will demonstrate through extensive numerical experiments that the treatment method mentioned here for micro-scale nodal forces is reasonable.

To derive the macroscopic equivalent forces, the principle of virtual work is used. As shown in Figs. 5 and 6a, the unit cell is in equilibrium if the microscopic forces virtual work equals the macroscopic forces virtual work for respective kinematically admissible displacement field. It can be expressed as:

$$\delta U = F_{\text{micro},n}\delta \mathbf{u}_n = F_{\mathbf{E},n}\delta \mathbf{u}'_{\mathbf{E}} \tag{18}$$

where $F_{\text{micro},n}$ is the force applied on the nth node of micro-scale meshes, $\delta \mathbf{u}_n$ is the virtual displacement vector of micro-scale node n, $\delta \mathbf{u}'_{\mathbf{E}}$ is the virtual displacement vector of macroscopic nodes of the unit cell, and $F_{\text{E},n}$ is the macroscopic equivalent forces that can be given in matrix form as follows:

$$F_{\mathbf{E},n} = [F_{\mathbf{E1},n}\ F_{\mathbf{E2},n}\ F_{\mathbf{E3},n}\ F_{\mathbf{E4},n}] \tag{19}$$

in which $F_{\mathbf{E}i,n} = [F_{\mathbf{E}ix,n}\ F_{\mathbf{E}iy,n}](i = 1, 2, 3, 4)$.

Using Eqs. 5, 7 and 9, we get

$$\mathbf{u}_n = \begin{Bmatrix} u_n \\ v_n \end{Bmatrix} = \begin{bmatrix} R_x(n) \\ R_y(n) \end{bmatrix} \{\mathbf{u}'_{\mathbf{E}}\} \tag{20}$$

By using Eqs. 18 and 20, we can obtain the macroscopic equivalent forces as follows:

$$F_{\mathbf{E},n} = F_{\text{micro},n} \times \begin{bmatrix} R_x(n) \\ R_y(n) \end{bmatrix} \tag{21}$$

Now, we discuss about the solution for microscopic perturbed forces (see Fig. 6b). From reference [34] we know that the boundary nodes of unit cell are deformed forcibly by the displacement of corresponding macroscopic nodes, while the internal nodes of unit cell are balanced automatically. To get the microscopic perturbed forces, boundary nodes are all constraint in x and y direction to be consistent with the constraint conditions shown in Fig. 3. Thus, the microscopic perturbed forces $f_{\text{perturbed,n}}$ can be obtained by the conventional FE analysis in fine-scale meshes under the constraint conditions mentioned above (see Fig. 6b).

Here, we present a one dimensional example to illustrate the validity of the equivalence of microscopic nodal forces. For the sake of simplicity, we assume that the truss structure contains only one unit cell and is composed of two truss elements with different cross sections (see Fig. 7). It is obvious that the nodes A, n and B are micro-scale nodes where the nodes A and B are also macro-scale nodes. The left endpoint of truss structure A is fixed in axial direction and a force $F_{\text{micro},n}$ is applied on the micro-scale node n. Elastic modulus E_e is used as the same in all examples in this paper with a magnitude of 1.0E6. The cross sections of two elements are 1 and 0.5, respectively. The length of two truss elements is both equal to 5.

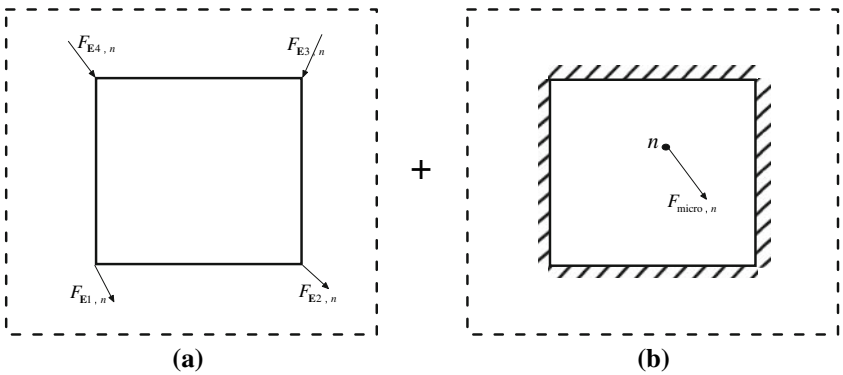

Fig. 6 Equivalence of micro-scale nodal force depicted in Fig 5: **a** Macroscopic equivalent forces; **b** Constrains for microscopic perturbed forces

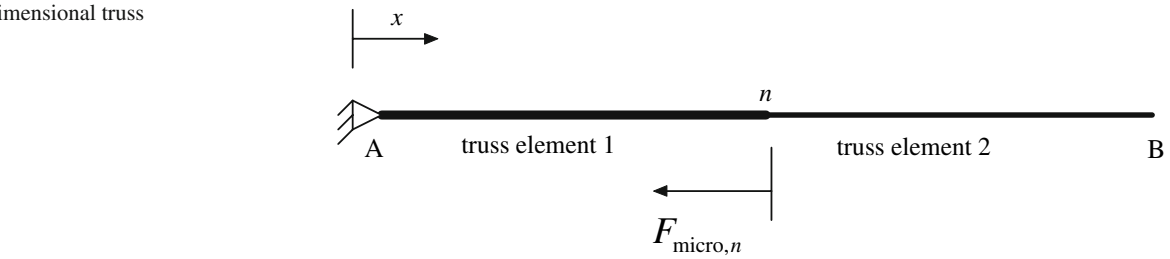

Fig. 7 A one-dimensional truss structure

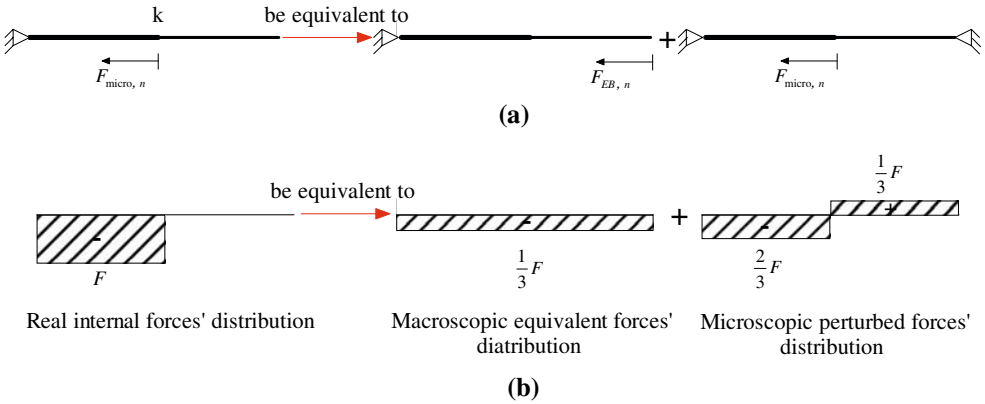

Fig. 8 Illustration of the equivalence of micro-scale nodal force: **a** the equivalent process and constraint conditions; **b** the internal forces' distribution of micro-elements under each force

It easy to construct the two numerical base functions of coarse element, they are $N_{Ax} = \left[1\ \frac{2}{3}\ 0\right]$ and $N_{Bx} = \left[0\ \frac{1}{3}\ 1\right]$, respectively. Then, using Eq. 21, we can obtain the macroscopic equivalent forces as follows:

$$F_{EA,n} = \frac{2}{3}F_{\text{micro},n}, \quad F_{\text{EB},n} = \frac{1}{3}F_{\text{micro},n}$$

Also, the microscopic perturbed forces induced by $F_{\text{micro},n}$ can be obtained when the endpoints A and B are all fixed. The equivalence process and boundary conditions are shown in Fig. 8a. Figure 8b shows the internal forces' distribution of micro-elements under each force. Note that a positive value implies tension and a negative value implies compression. From Fig. 8, we can see that the internal force distribution of each truss element obtained by the EMsFEM is consistent with real distribution. Meanwhile, it is easy to verify that the global displacement response obtained by macroscopic equivalent forces is equal to real situation.

4 EMsFEM for the elasto-plastic analysis of periodic truss material

4.1 Fundamental equations for the elasto-plastic multiscale computation

From the discussion above we can see that the micro-scale nodal forces can be approximately treated as the combined effects of macroscopic equivalent forces and microscopic perturbed forces. In this way, when the material nonlinear problems are considered in multiscale computation, the unbalanced nodal force $F_{\text{unbalanced},n}$ in micro-scale can be treated as $F_{\text{micro},n}$ and be dealt with in the same way.

For the truss elements in micro-scale, the strain increment is decomposed into elastic and plastic parts, $d\varepsilon^e$ and $d\varepsilon^p$, such that

$$d\varepsilon = d\varepsilon^e + d\varepsilon^p \tag{22}$$

and have following constitutive relations

$$d\sigma = E_e(d\varepsilon - d\varepsilon^p) \tag{23}$$

where $d\sigma$ is the micro stress increment and E_e is the elastic modulus of the truss element.

Moreover, the micro stress increment can be treated as the combined effects of two items, that is

$$d\sigma = d\sum + d\hat{\sigma} \tag{24}$$

where $d\sum$ is the stress increment induced by macroscopic equivalent forces $F_{\mathbf{E}}$ and $d\hat{\sigma}$ is the stress increment induced by microscopic perturbed forces $f_{\text{perturbed}}$. Note that $d\hat{\sigma}$ is set to zero for the first iteration step since there are no microscopic unbalanced forces exists at the moment.

It should be noted that in the EMsFEM the equivalent stiffness matrix of the unit cell is obtained by the base functions which are constructed numerically in micro-scale and depend on rigidity distribution of truss elements in the unit cell.

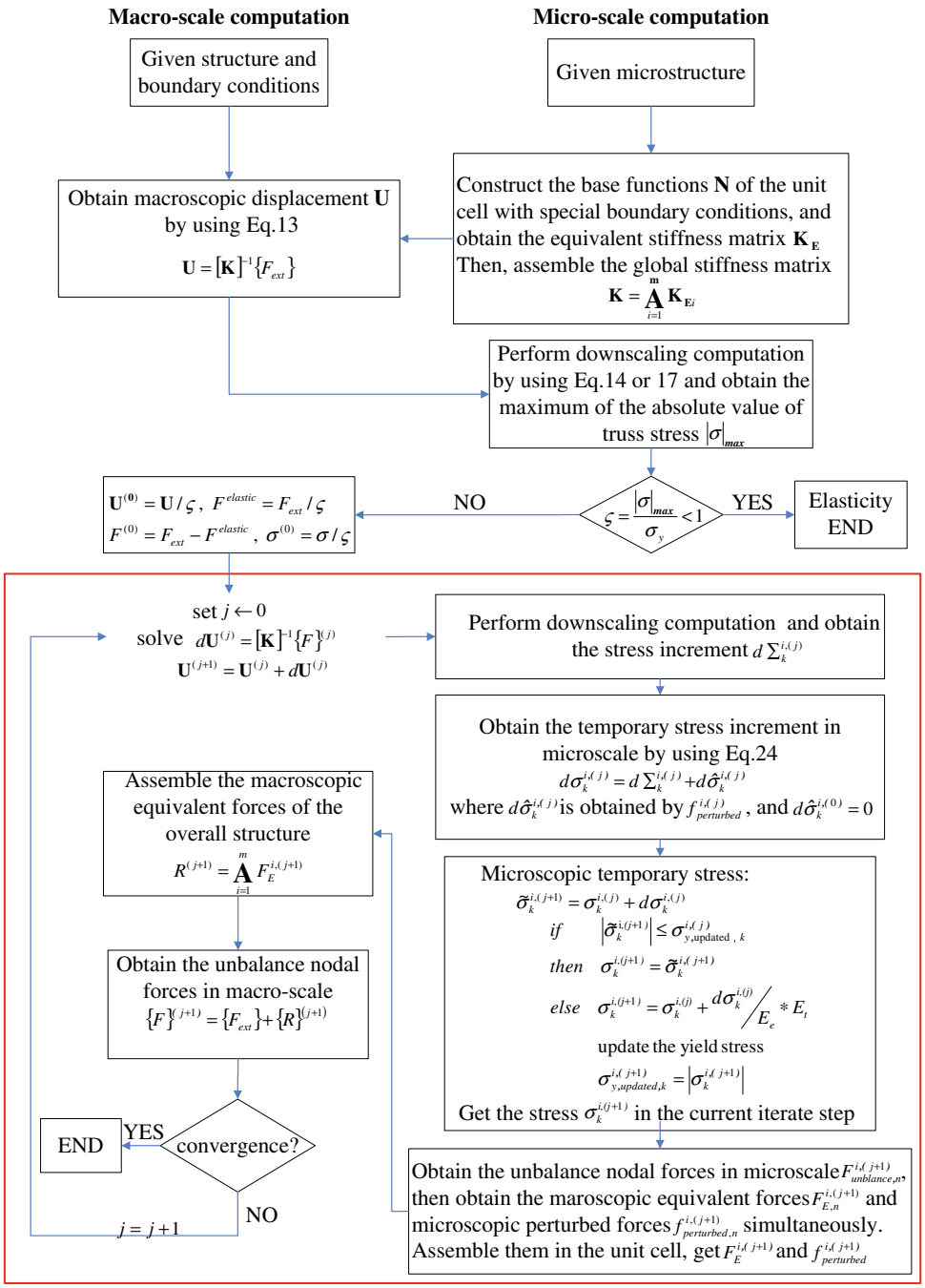

Fig. 9 Flow chart for multiscale elasto-plastic analysis of truss structures

In this context, the equivalent stiffness matrix will be changed along with the evolution of macroscopic deformation in elasto-plastic analysis. That is to say, for non-linear problems the base functions of each unit cell should be re-constructed, respectively, in different iteration steps and also the equivalent stiffness matrix of each unit cell should be re-obtained. It will cost too much computing efforts and become meaningless, unless the parallel computation is considered. In the present paper, the modified Newton–Raphson iterative procedures are used for both the micro- and macro-scale problems. In this way, the base functions and the equivalent stiffness matrices of the unit cells do not need to be changed. They are only computed for one time in the elastic stage and can be used for subsequent computations.

4.2 Flow chart for the elasto-plastic multiscale computation

The flow chart for the elasto-plastic multiscale analysis of truss structure is shown in Fig. 9. where σ_y is the initial yield stress, $\sigma_{y,\text{updated}}$ is the updated yield stress, E_e and E_t are the elastic and plastic moduli of truss elements, respectively. Here, in each step (j) for macroscopic iteration process, the

physical quantity of the kth truss element in the ith unit cell is denoted by $\bullet_k^{i,(j)}$. The algorithm is converged when macro- and micro-scale stress states are equilibrated simultaneously.

5 Numerical examples

In this section, several simple, but illustrative numerical examples are presented to examine the validity of the developed method. For comparison, the structures are also solved by the direct finite element method in fine-scale models (FEM-F), whose results can be regarded as reference solutions. For the last example, both linear boundary condition and oscillatory boundary condition are considered for the construction of base functions, and the numerical results obtained by the two boundary conditions are designated as EMsFEM-L and EMsFEM-O, respectively. In the following computation, we assume that the elastic-plastic behavior of truss material is described by bilinear isotropic hardening law. Moreover, all the truss elements have the following material properties: elastic modulus $E_e = 1.0\text{E}6$, plastic modulus $E_t = 0.3E_e$. All the numerical examples here are dimensionless.

Example 1 For the first numerical example, we consider the 1D truss structure presented in Sect. 3. As shown in Fig. 10, the total amount of macroscopic force $F_{\text{ext}} = 1,000$ is applied on the node B and is divided into 10 steps. The initial yield stress $\sigma_y = 1,500$. Figure 11 shows the macroscopic responses (i.e., displacement of the right-end of the macro-structure, Point B) to the increasing macroscopic external force. As can be seen from the figures, the EMsFEM give identical results compared to those of the FEM-F. Moreover, the micro-strains (i.e., the strains of truss elements 1 and 2) obtained by the EMsFEM at final loading step are 0.001 and 0.0032, respectively. It is also the same as reference solutions.

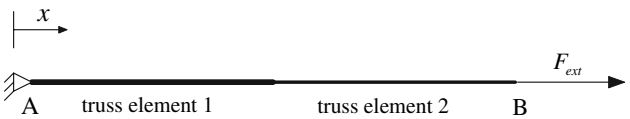

Fig. 10 A one-dimensional truss structure

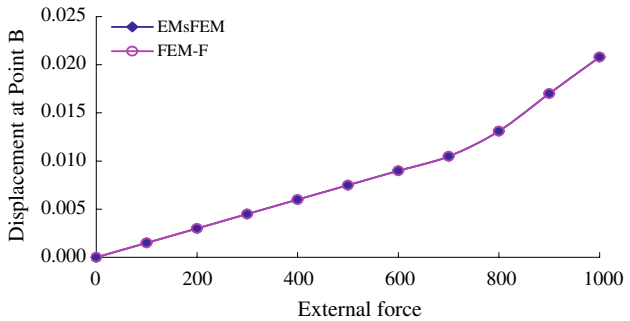

Fig. 11 Macroscopic load-displacement curves at Point B

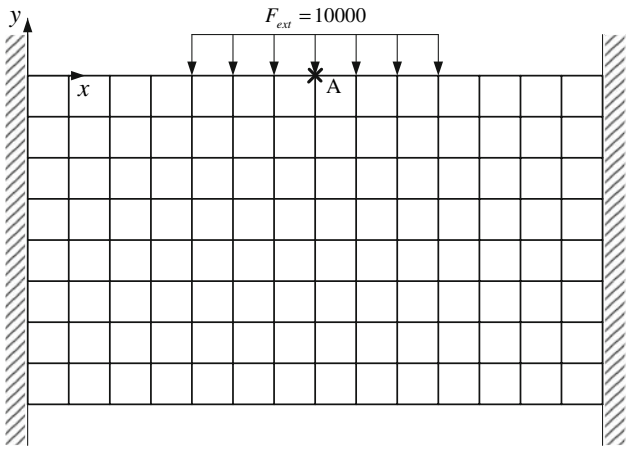

Fig. 12 Macroscopic FE model

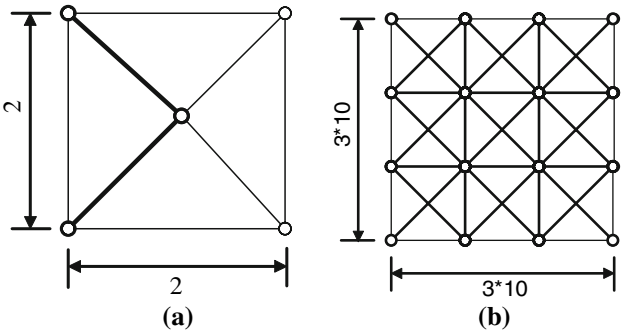

Fig. 13 Two kinds of unit cells: **a** unit cell 1 (Cross-section areas of the thinner truss elements are 0.2, while for the thicker ones, they are 1.0); **b** unit cell 2 (Cross-section areas of the outer elements are 0.5, while for internal elements, they are 1.0)

Example 2 Consider a macroscopic FE model shown in Fig. 12, which is composed of $n_x \times n_y = 14 \times 8$ unit cells, where n_x and n_y denote the number of unit cells in the x and y directions, respectively. The left and right sides of model are fixed in the two axis directions and a uniformly distributed load of 10,000 is applied on the top side and also divided into 10 steps. In this example, two kinds of unit cells are considered, respectively (see Fig. 13). For the unit cell 1, there are only two nodes at each boundary and the unit cell is heterogeneous. While for the unit cell 2, as the stiffness of truss elements within the unit cell are all the same, the unit cell is homogeneous. The initial yield stress of truss elements for two kinds of structures are set to $\sigma_y = 1,800$ and $\sigma_y = 150$, respectively. The base functions here are constructed with linear boundary condition. Fig. 14 shows the macroscopic load-displacement curves at Point A. As can be seen from figure, the EMsFEM yields almost the same results as the reference values when the unit cell 1 is considered. For the

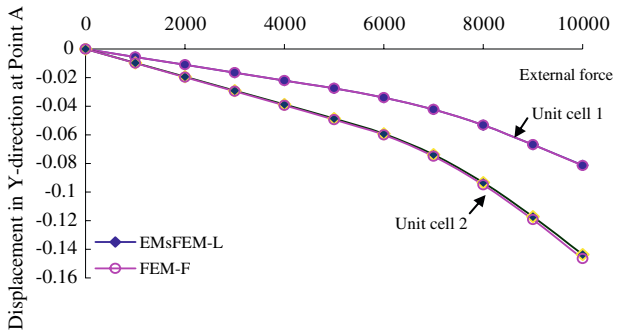

Fig. 14 Macroscopic load-displacement curves at Point A

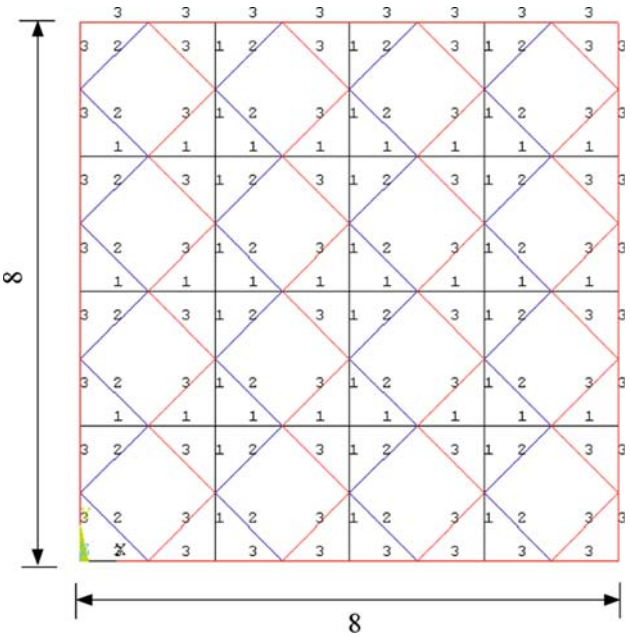

Fig. 15 A complicated heterogeneous unit cell (The cross-sections of three kinds of truss elements are 0.4, 1 and 0.2, respectively.)

heterogeneous unit cell with two nodes at each boundary, the boundary conditions do not affect the construction of base functions. In this case, the heterogeneity at the micro-level can be captured accurately by the base functions. For the structure composed of homogeneous unit cells (unit cell 2), the results obtained by the EMsFEM-L also fit fairly well with the reference values, the maximum relative error for the results obtained by the EMsFEM-L is less than 2% compared to those of the FEM-F. It illustrates that the base functions constructed with linear boundary condition are applicable to the homogeneous unit cell.

Example 3 For the macroscopic model shown in Fig. 12, the complicated heterogeneous unit cells are considered in this example. The sizes of truss elements within the unit cell are shown in Fig. 15. The initial yield stress of truss elements is set to $\sigma_y = 600$ here. Note that both the linear and oscillatory boundary conditions are considered here. Figure 16 shows

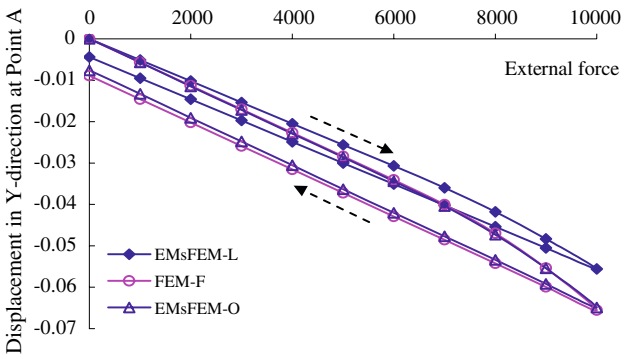

Fig. 16 Macroscopic load-displacement curves at Point A (The *dotted arrows* denote the loading and unloading direction)

the macroscopic load-displacement curves at Point A. From the results, we can see that the boundary conditions of the base functions have significant influence on the accuracy of the solutions for the heterogeneous materials. By comparing results between EMsFEM-L and EMsFEM-O, we see a great improvement in the accuracy of solutions using oscillatory boundary condition.

It is easy to know that the base functions constructed with linear boundary condition is established with forcing the boundary of the unit cell deformed linearly; these artificial constraints will induce unequilibrium nodal forces on the boundary and stiffen the structures, especially for strong heterogeneous materials. However, this boundary layer effect is not obvious for homogeneous unit cells. This is why the EMsFEM-L can obtain relatively good solutions for the unit cell 2 in the example 2. It can be further verified that if all the truss elements within the unit cell in Fig. 15 have the same cross-section area, then the results obtained by the EMsFEM-L will also agree well with the corresponding reference solutions. On other hand, since the oscillatory boundary condition can simulate the boundary deformation of unit cells more reasonably, the unequilibrium nodal forces on the boundary of unit cells can be reduced drastically. Thus, more accurate solutions will be obtained for the heterogeneous materials when the oscillatory boundary condition is used.

It should be remarked that a good choice of the boundary conditions can significantly improve the numerical precision of the multiscale method. In this paper, we just use the over-sampling technique to construct oscillatory boundary condition. There should be other types of boundary conditions that can be applied and may get improved accuracy. This investigation will be further done in our future work.

6 Computer memory and computing time comparison

The main purpose for developing multiscale methods is to solve some practical problems which are too large to handle

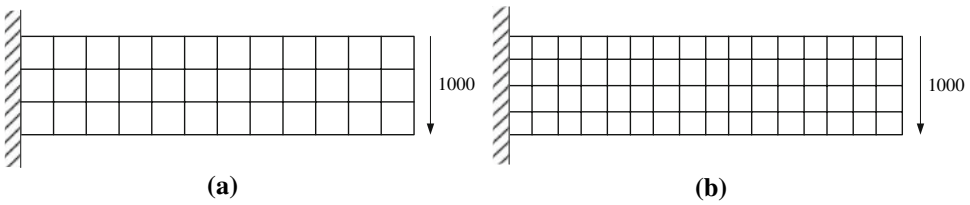

Fig. 17 Two kinds of macroscopic FE models: **a** macroscopic FE model 1; **b** macroscopic FE model 2

by direct methods even with modern supercomputers. As mentioned before, for most of existing multiscale methods, a complete micro RVE (unit cell) problem has to be solved at each Gauss point on the macro meshes in every iteration step. In this case, the deformation histories have to be stored and updated at every microscale element within the RVEs (unit cells) at all integration points for nonlinear history dependent systems. They still require enormous computational efforts when the structures are large. In our method, since the multiscale base functions are employed to establish the relationship between the macro and micro variables, the micro RVE problem is solved on macro meshes directly rather than at Gauss points of macro meshes, thus, the computational cost is further reduced. In this section, we make a rough estimate of the computer memory and CPU time in the EMsFEM, and compare them with those of the traditional FEM.

Let's consider a numerical model with the total number of nodes K. For FEM applied on the fine-scale model, the memory needed is $O(a \cdot K)$, where a is the number of degrees of freedom on a single node. For the 2-D truss structure considered in the present paper, $a = 2$. In the framework of EMsFEM, we assume that the number of nodes in macroscopic FE model and the number of nodes in micro-scale within each unit cell are N and M, respectively. In this context, if the serial computer is used, the memory needed for solving the problem on the coarse elements is $O(a \cdot N) + O(a \cdot M)$. It can be seen that when the structure is large (i.e., both the value of N and M are large), the memory needed is reduced significantly in our method. For the example 3, $N = 135, M = 65$, and $K = 5,553$. Then traditional FEM needs about 300 times more memory than EMsFEM.

For the material nonlinear problems, the operation count is $s_1 \cdot O(a \cdot K)$ for the FEM, where s_1 is the number of iterative steps. While for the EMsFEM, since the base functions and the equivalent stiffness matrix of unit cell of periodic material are only constructed for one time in the preprocessing computations and can be used for subsequent computations, a large amount of CPU time comes from solving microscopic perturbed forces and macro-scale FE computation. Thus the operation count of the EMsFEM is about $s_2 \cdot (O(a \cdot N) + N' \cdot O(a \cdot M))$, where s_2 is the number of iterative steps for the EMsFEM and N' is the number of coarse elements which is approximately equal to N. Note that both of the FEM and the EMsFEM use the modified Newton–Raphson iterative procedure for nonlinear analysis, the iterative steps are almost the same for the two methods. It should be mentioned that it is quit difficult to compare fairly the computing times between the EMsFEM and traditional FEM due to many factors (such as algorithm, hard ware, practical problems, etc), so the function expression of the operator 'O' is hard to define. But we can roughly estimate that it is the power of degrees of freedom if the serial computer is used. Thus, it also can be seen that the computing time is reduced significantly in our method when the structure is large.

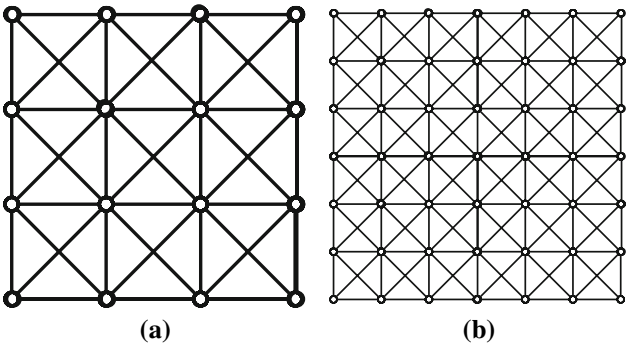

Fig. 18 Two kinds of unit cells: **a** Unit cell 1 (the same as the unit cell shown in Fig. 13b); **b** Unit cell 2 which is composed of 2×2 unit cell 1, and the sizes of elements in the unit cell are scaled by 1/2

Here, we present a numerical example to show the efficiency of the developed method. As shown in Fig. 17, two kinds of macroscopic FE models are considered, where the number of unit cells in the x and y directions are $n_x \times n_y = 12 \times 3$ for model 1 and $n_x \times n_y = 16 \times 4$ for model 2, respectively. The left side of the structure is fixed in the two axis directions and a uniformly distributed load is applied on right side. Meanwhile, two kinds of unit cells are considered (see Fig. 18), in which the unit cell 2 is composed of 2×2 unit cell 1. Table 1 shows the computing time comparison between the EMsFEM and the FEM for four different cases. It can be seen that the computing times for the FEM grow rapidly with the increasing of M and N. While for the EMsFEM, the computing times grow slowly. For the case 4 (i.e., the macroscopic FE model 2 and the unit cell 2 are adopted), our method only spends 3.8% computing time than the traditional FEM. In addition, if we solve a large structure that has $n_x \times n_y = 80 \times 20$ unit cells, and the

Table 1 computing time comparison (unit: s)

Macroscopic model	Unit cell style	EMsFEM	FEM
Macroscopic FE model 1	Case 1: unit cell 1	0.8	1.0
	Case 2: unit cell 2	2.7	23.2
Macroscopic FE model 2	Case 3: unit cell 1	1.6	3.2
	Case 4: unit cell 2	4.7	122.6

unit cell 2 is considered. Because the structure is too large, the direct FEM performed on fine-scale meshes (the program codes are written by commercial software Matlab) is hard to carry out due to large amount of degrees of freedom (a total of 116,402 degrees of freedom in fine scale). However, only about 101 s computing time are needed in the EMsFEM since the number of degrees of freedom is reduced drastically.

By the way, we would like to emphasize that, for the EMsFEM, the micro-scale problems are solved indepen dently on each coarse element; thus the EMsFEM can be easily extended for parallel computing. This will further reduce computational cost in solving the micro-scale problems. In this case, our method has great potential for nonlinear analysis of large random heterogeneous materials.

7 Conclusions

The algorithm of the EMsFEM for linear problems, which was proposed in reference [34], is generalized for elasto-plastic multiscale analysis of periodic truss structure. The base functions constructed numerically are employed to establish the relationship between the macroscopic displacement and the microscopic stress and strain. In macroscopic and microscopic iteration processes, the unbalanced nodal forces within the unit cells are treated as the combined effects of macroscopic equivalent forces and microscopic perturbed forces, in which the macroscopic equivalent forces are used to solve the macroscopic displacement field and the microscopic perturbed forces are used to obtain the stress and strain in the micro-scale. By means of this technique, a multiscale nonlinear analysis procedure is developed. From our numerical experiments we can see that the structural stiffness obtained by EMsFEM-L are overestimated for heterogeneous materials since the base functions constructed with linear boundary condition can not effectively reflect the boundary deformation of unit cells in the real physics phenomenon. Thus, the EMsFEM-O is introduced to overcome this problem. Numerical examples show that the results obtained by the developed method fit fairly well with those obtained by the direct FE method. Meanwhile, our method can reduce the CPU time and memory storage drastically for large structures.

In contrast to other homogeneous methods, the microscopic stress and strain information in the EMsFEM are obtained on macroscopic elements directly rather than at Gauss points of the elements. Thus, numerical data are not needed to be solved and updated at every integration points. Moreover, since the construction of base functions and micro-scale problems in the EMsFEM are performed on each coarse element independently; thus, the method developed here can be easily extended for the parallel computing. This gives hope to solving some large scale nonlinear problems of random heterogeneous materials that are intractable by traditional numerical methods. It should be noted that the method proposed here can also be used for solving dynamic problems, where the saving of computational time would be even more important. Further investigations will be carried out in our future work.

Acknowledgments The supports of the National Natural Science Foundation (10721062, 50679013, 90715037, 10728205), the 111 Project (No.B08014), the Program for Changjiang Scholars and Innovative Research Team in University (PCSIRT) and the National Key Basic Research Special Foundation of China (2010CB832704) are gratefully acknowledged.

References

1. Brittain ST, Sugimura Y, Schueller OJA, Evans AG, Whitesides GM (2001) Fabrication and mechanical performance of a mesoscale space-filling truss system. J Microelectromech Syst 10: 113–120
2. Huybrechts SM, Meink TE, Wegener PM, Ganley JM (2002) Manufacturing theory for advanced grid stiffened structures. Compos Appl Sci Manuf 33:155–161
3. Hou A, Gramoll K (1998) Compressive strength of composite lattice structures. J Reinforce Plast Compos 17:462–483
4. Deshpande VS, Ashby MF, Fleck NA (2001) Foam topology: bending versus stretching dominated architectures. Acta Materialia 49:1035–1040
5. Wallach JC, Gibson LJ (2001) Mechanical behavior of a three-dimensional truss material. Int J Solids Struct 38:7181–7196
6. Budiansky B (1965) On the elastic moduli of some heterogeneous materials. J Mech Phys Solids 13:223–227
7. Chen HS, Acrivos A (1978) The effective elastic moduli of composite materials containing spherical inclusions at non-dilute concentrations. Int J Solids Struct 14:349–364
8. Nemat-Nasser S, Hori M (1993) Micromechanics: overall properties of heterogeneous materials. North-Holland, Amsterdam

9. Kouznetsova V (2002) Computational homogenization for the multi-scale analysis of multi-phase materials. PhD-thesis, Technical University of Eindhoven, Eindhoven
10. Pecullan S, Gibiansky LV, Torquato S (1999) Scale effects on the elastic behavior of periodic and hierarchical two-dimensional composites. J Mech Phys Solids 47:1509–1542
11. Noor AK (1988) Continuum modeling for repetitive lattice structures. Appl Mech Rev 41:285–296
12. Gonella S, Ruzzene M (2008) Homogenization and equivalent in-plane properties of two-dimensional periodic lattices. Int J Solids Struct 45:2897–2915
13. Suiker ASJ, Metrikine AV, de Borst R (2001) Comparison of wave propagation characteristics of the cosserat continuum model and corresponding discrete lattice models. Int J Solids Struct 38: 1563–1583
14. Benssousan A, Lions JL, Papanicoulau G (1978) Asymptotic analysis for periodic structures. North-Holland, Amsterdam
15. Paumelle P, Hassim F, Lene F (1991) Microstress analysis in woven composite structures. Rech Aerospatiale 6:47–62
16. Lee K, Moorthy S, Ghosh S (1999) Multiple scale computational model for damage in composite materials. Comput Meth Appl Mech Eng 172:175–201
17. Oskay C, Fish J (2008) On calibration and validation of eigendeformation-based multiscale models for failure analysis of heterogeneous systems. Comput Mech 42:181–195
18. Terada K, Kikuchi N (1995) Nonlinear homogenization method for practical applications. In: Ghosh S, Ostoja-Starzewski M (eds) Computational Methods in Micromechanics, AMSE AMD, vol 212, pp 1–16
19. Fish J, Shek K, Pandheeradi M, Shephard M (1997) Computational plasticity for composite structures based on mathematical homogenization: theory and practice. Comput Meth Appl Mech Eng 148:53–73
20. Terada K, Hori M, Kyoya T, Kikuchi N (2000) Simulation of the multi-scale convergence in computational homogenization approaches. Int J Solids Struct 37:2285–2311
21. Matsui K, Terada K, Yuge K (2004) Two-scale finite element analysis of heterogeneous solids with periodic microstructures. Comput Struct 82:593–606
22. Kouznetsova V, Brekelmans WAM, Baaijens FPT (2001) An approach to micro-macro modeling of heterogeneous materials. Comput Mech 27:37–48
23. Babuska I, Osborn E (1983) Generalized finite element methods: Their performance and their relation to mixed methods. SIAM J Numer Anal 20:510–536
24. Babuska I, Caloz G, Osborn E (1994) Special finite element methods for a class of second order elliptic problems with rough coefficients. SIAM J Numer Anal 31:945–981
25. Hou TY, Wu XH (1997) A multiscale finite element method for elliptic problems in composite materials and porous media. J Comput Phys 134:169–189
26. Hou TY (2005) Multiscale modelling and computation of fluid flow. Int J Numer Meth Fluid 47:707–719
27. Efendiev Y, Ginting V, Hou TY, Ewing R (2006) Accurate multiscale finite element methods for two-phase flow simulations. J Comput Phys 220:155–174
28. Aarnes JE (2004) On the use of a mixed multiscale finite element method for greater flexibility and increased speed or improved accuracy in reservoir simulation. Multiscale Model Sim 2:421–439
29. Aarnes JE, Krogstad S, Lie KA (2006) A hierarchical multiscale method for two-phase flow based upon mixed finite elements and nonuniform coarse grids. Multiscale Model Sim 2:421–439
30. Dostert P, Efendiev Y, Hou TY (2008) Multiscale finite element methods for stochastic porous media flow equations and application to uncertainty quantification. Comput Meth Appl Mech Eng 197:3445–3455
31. Jenny P, Lee SH, Tchelepi HA (2003) Multi-scale finite volume method for elliptic problems in subsurface flow simulation. J Comput Phys 187:47–67
32. Ginting V (2004) Computational upscaled modeling of heterogeneous porous media flows utilizing finite volume method. PHD thesis, Texas A & M University, College Station
33. Zhang HW, Fu ZD, Wu JK (2009) Coupling multiscale finite element method for consolidation analysis of heterogeneous saturated porous media. Adv Water Resour 32:268–279
34. Zhang HW, Wu JK, Fu ZD (2010) Extended multiscale finite element method for mechanical analysis of periodic lattice truss materials. Int J Multiscale Com (accepted)
35. Ye HF, Wang JB, Zhang HW (2009) Numerical algorithms for prediction of mechanical properties of single-walled carbon nanotubes based on molecular mechanics model. Comp Mater Sci 44: 1089–1097